Available online at www.sciencedirect.com

SCIENCE DIRECT

Solid State Ionics 176 (2005) 1393 – 1401

SOLID STATE IONICS

www.elsevier.com/locate/ssi

Transport properties of $Li_2O–MnO_2–B_2O_3$ glasses

V.C. Veeranna Gowda, R.V. Anavekar*

Department of Physics, Bangalore University, Bangalore-560 056, India

Received 3 January 2005; received in revised form 16 March 2005; accepted 4 April 2005

Abstract

Lithium borate containing MnO_2 glasses have been synthesized by melt quenching technique over a wide composition range. Frequency and temperature dependent conductivity measurements have been carried out in the range of 10 Hz to 13 MHz and at a temperature range of 298 K–523 K respectively. The impedance plots show only one semicircle indicating the presence of one type of conduction mechanism. The analysis of dc conductivity show that the conductivity is dominated by Li^+ ions and the presence of MnO_2 has negligible effect. The ac conductivity data has been analysed by fitting the data into Almond-West type power law behaviour $\sigma = \sigma(o) + A\omega^s$. The power law exponent s is also determined and it is found to decrease with increase of temperature. We have also carried out the scaling behaviour of the ac conductivity and it is seen that all the curves coalesce on to a master curve suggesting that the ion transport mechanism remains unaffected at all temperatures. The results are discussed in the light of the structure of borate glass network.

Keywords: Borate glasses; AC conductivity; Scaling; Dielectric relaxation; Li^+ conduction

1. Introduction

The transport properties of oxide glasses have been of interest for a long time because of their potential applications in technology. The use of glasses both as electrolyte and electrode materials has given a boost to the study of ion transport in glasses and search for new glassy materials. Lithium borates are classical glass forming systems, which have been extensively studied in the literature [1–3]. The ability of boron to exist in both three and four coordinated environments and high strength of the covalent B–O bonds, imparts borates, the ability to form stable glasses. It is well known that lithium ion conducting batteries develop high voltages and high energy density due to their light weight and highly electropositive character of the lithium metal. These glasses have several advantages over crystalline counterparts; easy formability over a wide range of composition, isotropicity, absence of grain boundaries, ease of fabrication into complex shapes.

The mechanism of electrical conductivity in ion conducting glasses is a challenging problem. The conductivity is generally studied as a function of temperature, and it may also depend on structural changes in the material. This point of view is interesting because the conductivity of vitreous material is caused by at least two different contributions. The first one is thermal activation. The conductivity increases with temperature according to the Arrhenius law. The second one is the structural change of the glass with composition, which also causes a variation of conductivity [4,5]. Therefore it is interesting to understand the dynamics of the mobile ions in solid ion conductors by interpreting the frequency dependent features in their dielectric response [6,7]. Lithium borate glasses containing transition metal ions such as manganese and nickel are known for electrode materials. In the literature, we find that these glasses have not been studied extensively. In an effort to understand the conductivity behaviour and to find some universality in them, $Li_2O–MnO_2–B_2O_3$ glass system has been taken up for investigation.

Here, we report both dc and ac conductivity studies performed on $Li_2O–MnO_2–B_2O_3$ glasses over a wide range of composition, temperature and frequency. Interest-

* Corresponding author. Tel.: +91 80 23214001x332; fax: +91 80 23389295.

E-mail address: anavekar_271@yahoo.co.in (R.V. Anavekar).

0167-2738/$ - see front matter © 2005 Elsevier B.V. All rights reserved.
doi:10.1016/j.ssi.2005.04.002

ingly, it is found that the conductivities are dominated by lithium ions and the structure of borate glass. The scaling analysis exhibits excellent collapse of conductivity and dielectric modulus (M'') on to single master curve suggesting a common transport mechanism in this glass system.

2. Experimental

The binary $Li_2O–B_2O_3$ and ternary $Li_2O–MnO_2–B_2O_3$ glasses have been synthesised using high purity analar grade chemicals lithium carbonate (Li_2CO_3), manganese dioxide (MnO_2) and orthoboric acid (H_3BO_3). Mixtures of these materials in appropriate proportions were taken in porcelain crucibles and thoroughly mixed and melted in a crucible at about 1200 °C to get a homogeneous melt. The glasses suitable for electrical conductivity measurements were prepared by melt quenching method. All the samples were annealed below their transition temperature.

Electrical conductivity measurements were carried out on a Hewlett Packard HP 4192A impedance gain phase analyzer from 10 Hz to 13 MHz in the temperature range of 298 K to 523 K. A home built cell assembly (2-terminal capacitor configuration and spring loaded silver electrodes) was used for all measurements. The sample temperature was measured using a Pt–Rh thermocouple positioned very close to the sample. The temperature was controlled using a Heatcon (Bangalore, India) temperature controller and the temperature constancy of ± 1 K was achieved in the entire range of measurements. Annealed circular glass pieces, coated with silver paint on both sides and having thickness of about 0.1 cm and a diameter of 1 cm were used for the measurements.

3. Analysis of data

The capacitance (C_p) and conductance (G) of all the samples were measured from the impedance analyser. These were used to evaluate the real and imaginary parts of the complex impedance using standard relations

$$Z^* = Z' + jZ'' = \frac{1}{(G + j\omega C_p)} \tag{1}$$

$$Z' = \frac{G}{\left(G^2 + \omega^2 C_p^2\right)} \tag{2}$$

$$Z'' = \frac{\omega C_p}{\left(G^2 + \omega^2 C_p^2\right)} \tag{3}$$

The dc conductances were determined from the semicircular complex impedance (Z' versus Z'') plots by taking the value of intersection of the low frequency end of the semicircle on Z' axis. The conductivity (σ) for each sample was calculated using the expression

$$\sigma = G\left(\frac{d}{A}\right) \tag{4}$$

where d and A are the thickness and area of the sample respectively.

The real (ε') and imaginary (ε'') parts of the complex dielectric constant were calculated from the relations,

$$\varepsilon' = \frac{C_p d}{A\varepsilon_0} \tag{5}$$

$$\varepsilon'' = \frac{\sigma}{\varepsilon_0 \omega} \tag{6}$$

where ε_o is the permittivity of the free space.

The data were also analysed using the electrical modulus formalism [8]. The real (M') and imaginary (M'') parts of the complex electrical modulus ($M^* = 1/\varepsilon^*$) were obtained from ε' and ε'' values using the relations,

$$M' = \frac{\varepsilon'}{\left(\varepsilon'^2 + \varepsilon''^2\right)} \tag{7}$$

$$M'' = \frac{\varepsilon''}{\left(\varepsilon'^2 + \varepsilon''^2\right)} \tag{8}$$

4. Results and discussion

Compositions of the glasses studied and their corresponding codes are listed in Table 1. The impedance plots of

Table 1
Compositions of the glasses prepared, along with codes of designation and their corresponding σ_{dc}, s, and β at K, E_{dc} and E_{ac}

Code	Composition (mol%)			σ_{dc}, S cm^{-1}	s	β	E_{dc}, eV	E_{ac}, eV
	Li_2O	MnO_2	B_2O_3					
LB1	10	0	90	5.28×10^{-8}	0.53	0.55	1.03	1.01
LB2	20	0	80	1.32×10^{-7}	0.55	0.54	0.99	0.98
LB3	30	0	70	4.98×10^{-6}	0.59	0.50	0.81	0.79
LB4	40	0	60	2.00×10^{-5}	0.59	0.57	0.77	0.73
CM1	5	15	80	–	–	–	–	–
CM2	10	15	75	2.76×10^{-7}	0.55	0.62	1.03	0.96
CM3	15	15	70	2.39×10^{-8}	0.57	0.59	1.01	0.95
CM4	20	15	65	2.45×10^{-9}	0.58	0.60	0.97	0.96
CM5	25	15	60	9.24×10^{-7}	0.66	0.58	1.01	0.97
CM6	30	15	55	1.91×10^{-6}	0.48	0.56	0.98	0.93
CL1	15	5	80	–	–	–	–	–
CL2	15	10	75	1.39×10^{-8}	0.56	0.59	1.02	0.90
CL3	15	15	70	2.39×10^{-8}	0.57	0.60	1.05	0.98
CL4	15	20	65	4.17×10^{-8}	0.48	0.56	0.98	0.95
CL5	15	25	60	1.72×10^{-8}	0.57	0.59	0.91	0.87
CL6	15	30	55	2.54×10^{-8}	0.54	0.59	0.94	0.89
CB1	5	35	60	–	–	–	–	–
CB2	10	30	60	1.05×10^{-8}	0.61	0.59	1.07	1.01
CB3	15	25	60	1.71×10^{-8}	0.57	0.60	1.12	1.05
CB4	20	20	60	1.61×10^{-7}	0.55	0.58	1.09	1.01
CB5	25	15	60	9.24×10^{-7}	0.52	0.57	1.00	0.98
CB6	30	10	60	3.49×10^{-6}	0.47	0.60	0.95	0.90
CB7	35	5	60	2.01×10^{-5}	0.43	0.58	0.91	0.89

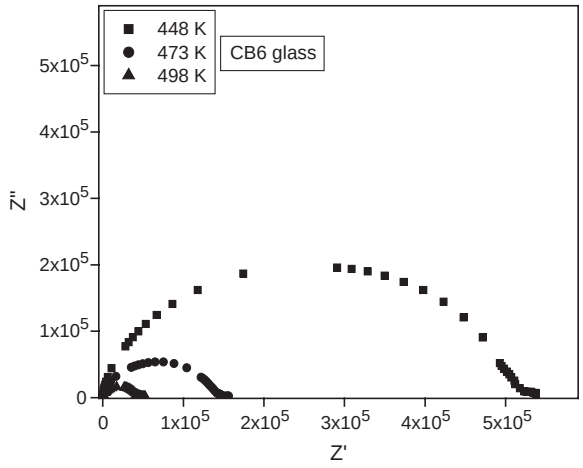

Fig. 1. Typical impedance plots for CB6 glass at different temperatures.

all the samples were found to exhibit good semicircles. A typical impedance plots for CB6 glass at different temperatures is shown in Fig. 1. In all the samples, only one semicircle has been observed over the entire range of temperature studied. The dc conductivities were calculated by taking the intersection points of the semicircle on real axis. The intersection points of the semicircles shifted to lower and lower Z' values with increasing temperature. The variation of dc conductivities as a function of temperature for LB, CL, CM and CB series of glasses are shown in Fig. 2a–d. In all the glasses, single linear variation of $\log(\sigma)$ versus $1000/T$ has been observed.

5. DC conductivity

Fig. 2a shows the Arrhenius plots of dc conductivity of binary lithium borate glasses. It is clear from Fig. 2a that the dc conductivity progressively increases as the Li_2O concentration is increased. This is expected, since the lithium ions are the main charge carriers [9–12]. Fig. 2b shows the Arrhenius plot of dc conductivity for CL glass series. As can be seen from Fig. 2b that the dc conductivity seem to be almost independent of MnO_2 concentration indicating that the presence of MnO_2 does not contribute much to the conductivity. The constancy of conductivity in CL series may also indicate that the lithium ions present in the glass system weakly interact with the B–O network structure.

In CM glass series also the conductivity follow the Arrhenius behaviour (Fig. 2c). But the conductivity decreases with increase of Li_2O concentration up to 20 mol%. Further

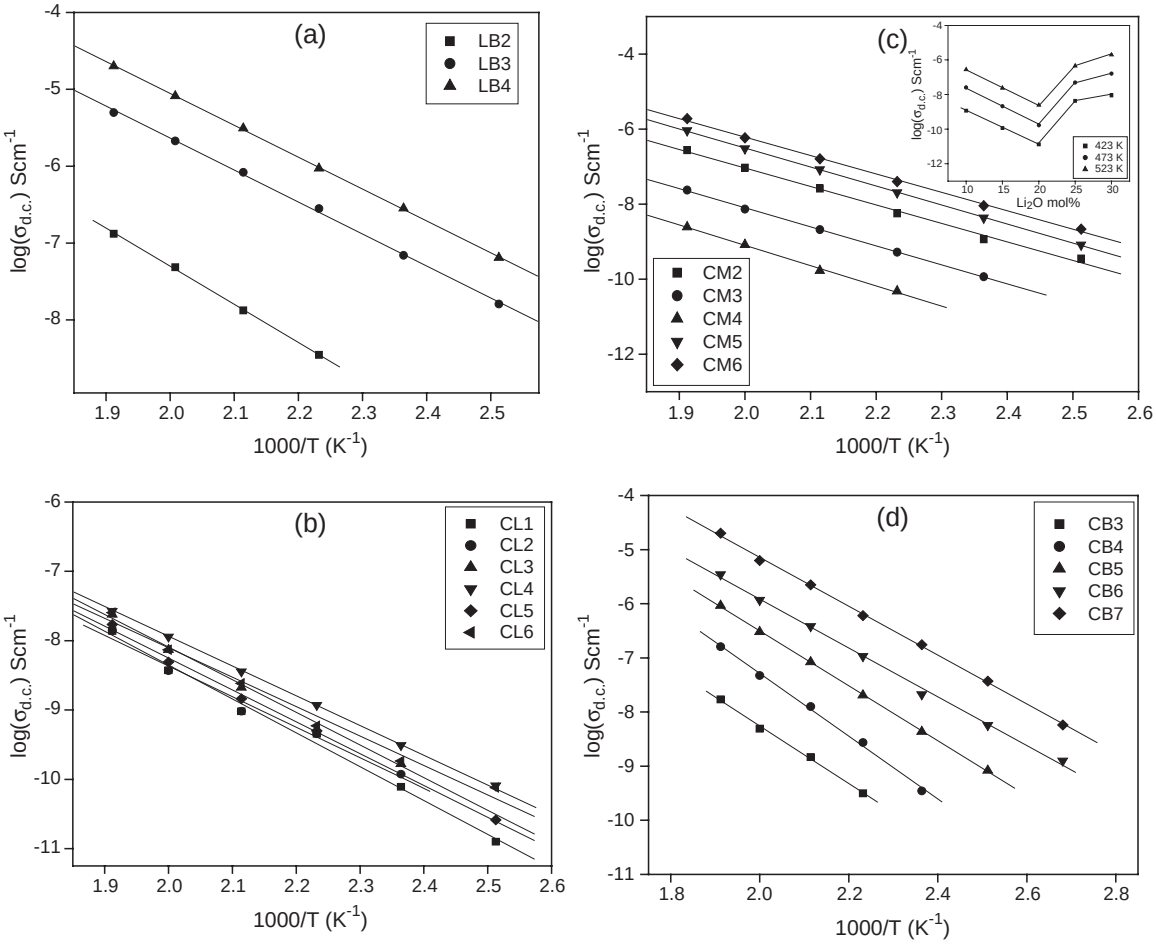

Fig. 2. a–b. Variation of $\log(\sigma_{dc})$ versus $1000/T$ for (a) LB and (b) CL glass series. c–d. Variation of $\log(\sigma_{dc})$ versus $1000/T$ for (c) CM and (d) CB glass series.

addition of Li_2O concentration leads to an increase in conductivity by two orders of magnitude (see isothermal plot given in the inset of Fig. 2c). Such behaviour is likely to arise due to the structural changes occurring in borate glass network. In binary $Li_2O-B_2O_3$ glasses, the addition of one mol% of Li_2O will convert two moles of $[BO_{4/2}]^-$ (gB_4) units at the expense of $[BO_{3/2}]^o$ (gB_3) unit. This process continues till the concentrations of $B_3=B_4$ i.e., the diborate composition (when the modifier concentration is approximately 33 mol%). Further increase in modifier concentration leads to reconversion of B_4 to $[BO_{2/2}O]^-$ (gB_2) unit with a non bridging oxygen. In the present glass system, when the effective modifier concentration (Li_2O+MnO_2) is greater than 33 mol% leads to reconversion of B_4 to B_2 units. Due to the creation of non-bridging oxygens, the openness of the network results in the weakening of the borate structure. This is likely to facilitate greater mobility of Li^+ ions resulting to an increase in conductivity.

The behaviour of conductivity in CB glass series is similar to that is observed in binary lithium borate glasses and it is shown in Fig. 2d. The conductivity in CB series increases up to three orders of magnitude when the Li_2O concentration is increased from 5 to 35 mol%. This is expected, since Li_2O is substituted in place of MnO_2. As in LB series, the migrations of Li^+ ions are responsible for the increased conductivity in CB glass series [12].

Interestingly, the magnitude of conductivity in both LB and CB glass series is of the same order (10^{-5}–10^{-8} S cm^{-1}) which clearly indicates that the presence of MnO_2 has negligible effect on lithium ion motion and does not contribute to electronic conductivity. It is known that the alkali oxide glasses containing transition metal oxide exhibit mixed conductivity. For example, in $Na_2O-B_2O_3-V_2O_5$ glasses, the contribution to conductivity is both electronic and ionic [13]. This would result in a non-linear variation of conductivity behaviour. But in the present glass system such a non-linear behaviour of conductivity has not been observed. This clearly reveals that the conductivity in the present glass system is only due to the motion of Li^+ ions.

The activation energies calculated from regression analysis of $\log(\sigma)$ versus $1000/T$ plots are listed in Table 1. In the case of LB and CB series of glasses, the activation energy decreases with increase of Li_2O concentration where as in case of CL and CM series, the activation energies are almost equal suggesting the fact that the lithium ions have same environment in the glass network.

6. AC conductivity behaviour

A typical plot of ac conductivity as a function of frequency for CB6 glass is shown in Fig. 3a. The ac conductivity behaviour of all the other glasses is qualitatively similar. The ac conductivities exhibit a change of slope to higher values as the frequency is increased. A nearly flat portion at lower frequencies and an increase to higher values of conductivity at higher temperatures. The ac conductivity has been analysed using Almond-West type power law with single exponent [14–16]

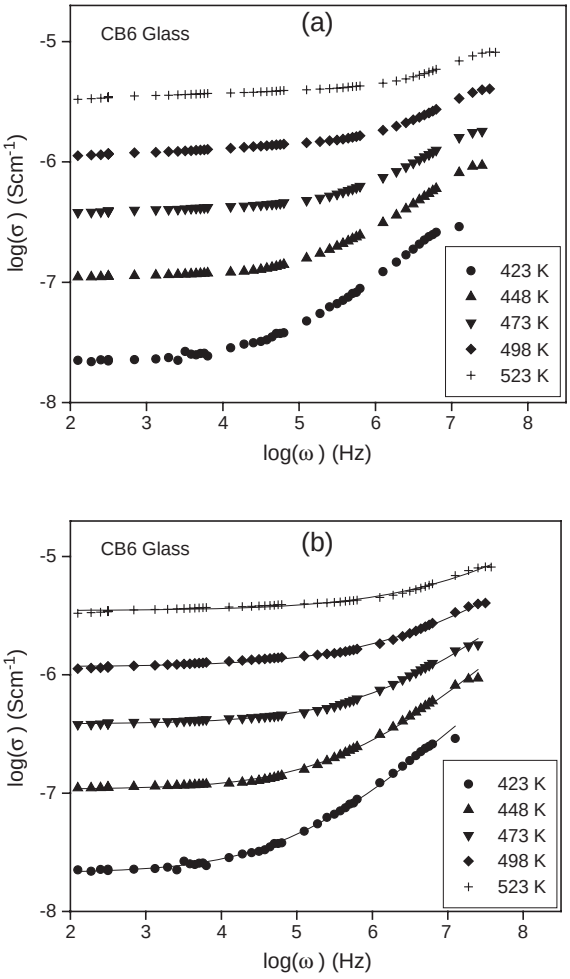

Fig. 3. (a) Variation of $\log(\sigma)$ versus frequency and (b) typical ac conductivity plots fitted to the power law equation for CB6 glass at different temperature.

$$\sigma(\omega) = \sigma_o + A\omega^s \tag{9}$$

where σ_o is frequency independent and it is identified with the dc conductivity and the second term is the purely dispersive component of the ac conductivity, depending on the frequency ω ($\omega=2\pi f$ is the angular frequency) in a characteristic power law fashion. A and s are power law fit parameters. The power law exponent s has been found to be material dependent [17]. Typical ac conductivity fit to Almond-West type power law is shown in Fig. 3b for CB6 glass. At low frequencies, random distribution of the ionic charge carriers via activated hopping gives rise to a frequency independent conductivity. At higher frequencies, conductivity exhibits dispersion, increasing roughly in a power law fashion and eventually becoming almost linear at even higher frequencies [18]. It is also evident from Fig. 3b that the power law fit is remarkably good throughout the frequency regime and therefore single exponent fit seems to

Table 2
The code of the glass sample, power law fit parameters, A and χ^2 values at 523 K for CB glass series

Code	A	χ^2
CB2	9.85×10^{-11}	0.00016
CB3	8.78×10^{-11}	0.00009
CB3	2.88×10^{-10}	0.00011
CB5	2.06×10^{-10}	0.00019
CB6	1.62×10^{-9}	0.00004
CB7	1.02×10^{-9}	0.00001

be adequate. Another interesting feature observed is that the values of σ_o obtained from the Almond West type power law fit are similar in magnitude to the dc conductivities (σ_{dc}) obtained from the impedance plots.

The power law exponent, s obtained from power law fit is listed in Table 1. The typical power law fit parameters (A and $\chi 2$) of one of the glass (CB) series are given in Table 2. The behaviour of s as a function of temperature for each material is investigated and it has been found that for all the glasses s values are temperature dependent and significantly lower than unity and generally lie in a narrow range of 0.5–0.7 [17]. But in case of CB glasses, s values lie between 0.42 and 0.63. The variation of s values with temperature for all the glass series is shown in Fig. 4a–d and it is clearly seen that s values are high at low temperature and decrease with increase of temperature. The dispersion of s values is somewhat higher at higher temperatures. It is also evident from Fig. 4c is that the variation of s in CM series is marginal. This indicates the presence of least modification in the network structure. In CB glass series lowest s value has been observed. In these glasses s is significantly high at low temperature. The lowest s value appears to be associated with high degree of modification. Further, s values are strongly dependent on the concentration of modifier oxide; higher Li_2O content glasses have lower s values. Such behaviour is often attributed to the inter-lithium ion interactions influencing the ac transport [13,19,20]. Although, the analysis of Almond-West type power law equation is limited by an inherent ''window effect''. However, the observed change in the exponent generally remains within the error of determination (± 5%) and renders the window effect much less important than it appears to be [21–23].

The values of activation energies, E_{dc} determined from $\log(\sigma)$ versus $1000/T$ plots are given in Table 1. The activation energies in case of binary lithium borate glasses

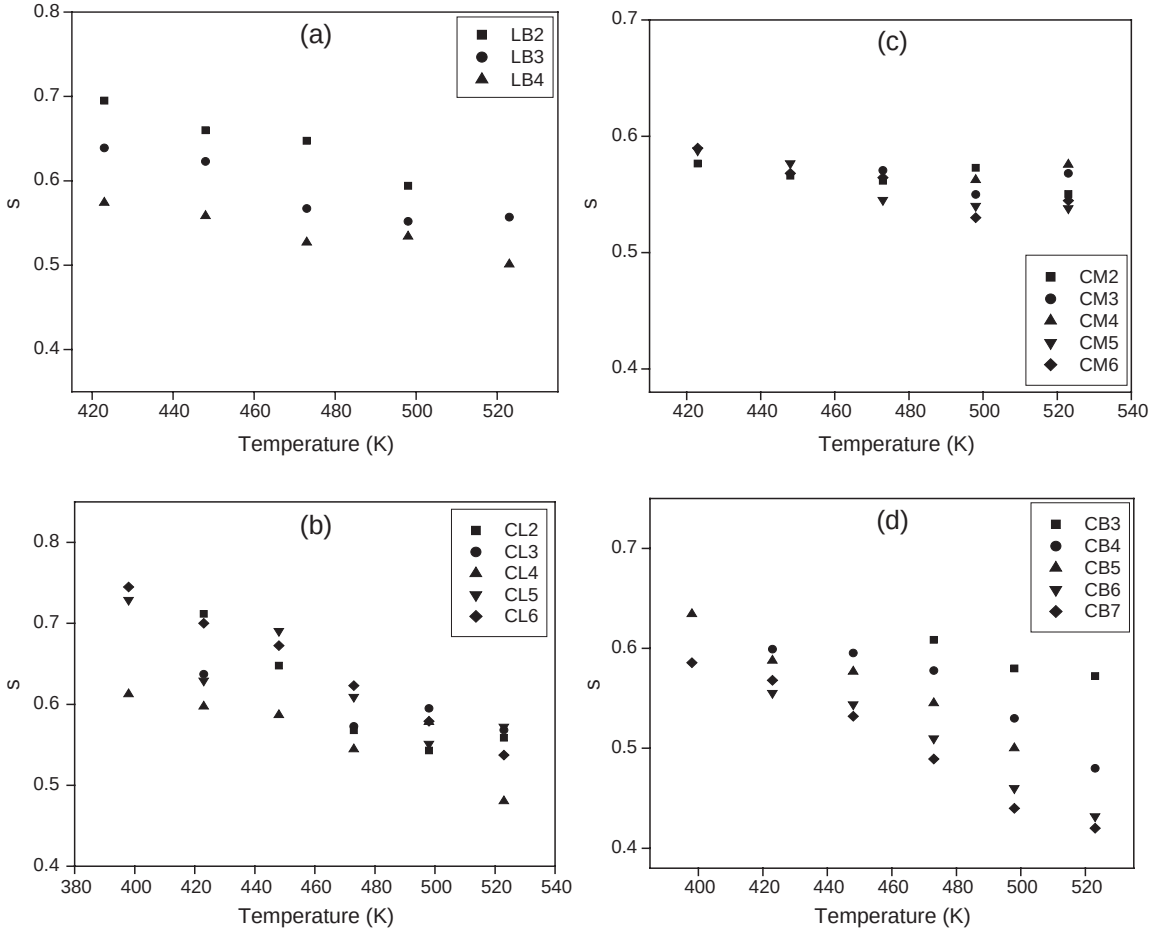

Fig. 4. a–b. Variation of power law exponent s with temperature for (a) LB and (b) CL glass series. c–d. Variation of power law exponent s with temperature for (c) CM and (d) CB glass series.

decrease with increase of Li_2O concentration and these are in good agreement with those reported in the literature [9–11]. The decrease in activation energy in such glasses is explained on the basis of Anderson–Stuart model [24], which considers the activation energy is the sum of both electrostatic binding energy and strain energy. The low activation energies in LB series leads to higher conductivity as the concentration of Li_2O increases due to the contribution of large number of lithium ions, since lithium ions are highly mobile and significantly increase the electrical conductivity of the system. The activation energies of LB glasses are quite small compared to the activation energies of MnO_2 containing glasses. The high activation barriers in MnO_2 based glasses may be due to the fact that greater numbers of Li^+ ions in these glasses are surrounded by oxygen ions from borate groups.

7. Dielectric relaxation

The dielectric response of these glasses have been examined by measuring both real and imaginary parts of the dielectric constants and moduli in the range of 10 Hz to 13 MHz. The variation of real (ε') and imaginary (ε'') parts of dielectric constant with frequency for CB6 glass at different temperature is shown in Fig. 5a and b. Since the glasses investigated are ion conducting; low frequency dispersion is quite high which is generally attributed to

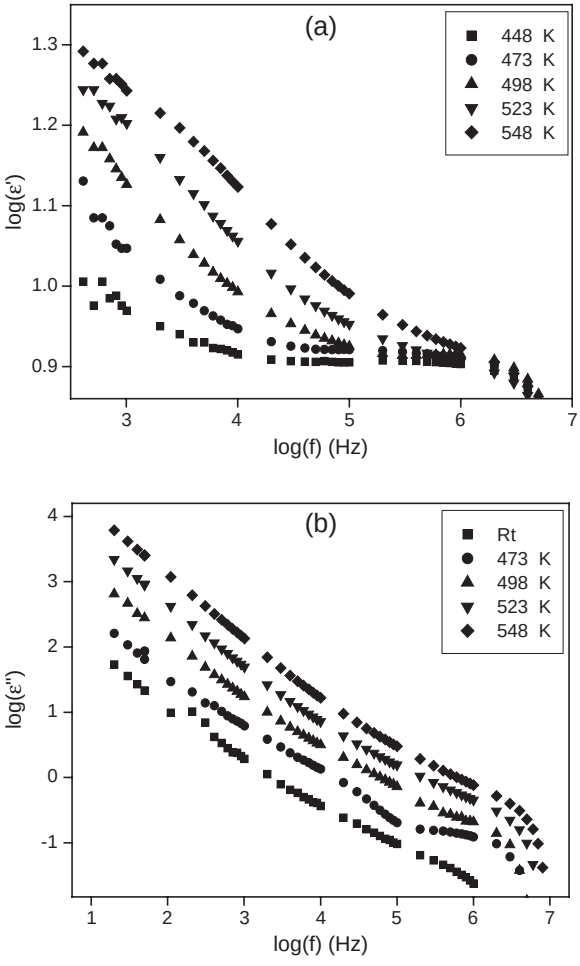

Fig. 5. Typical plots of variation of (a) real (ε') and (b) imaginary (ε'') parts of the dielectric constant with frequency for CB6 glass at different temperatures.

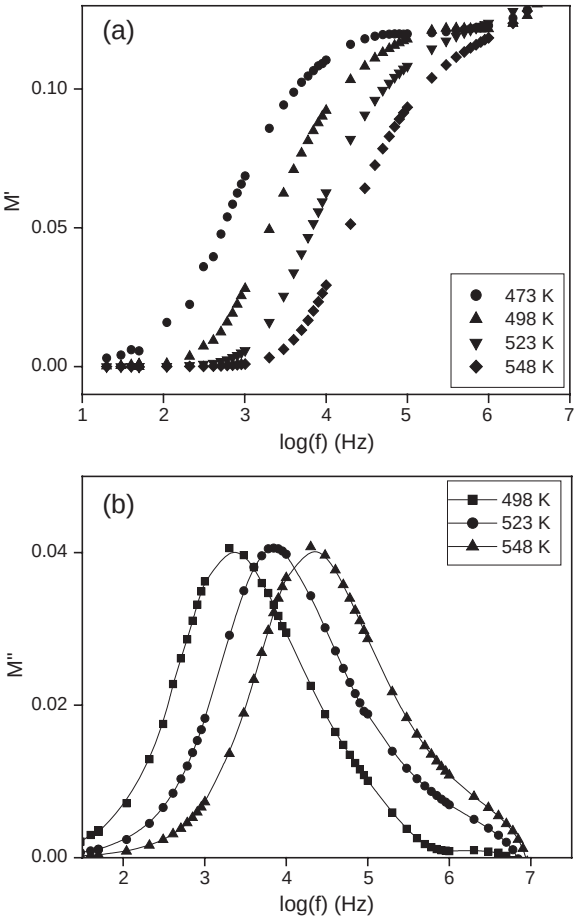

Fig. 6. Typical plots of variation of (a) real (M') and (b) imaginary (M'') parts of the dielectric modulus with frequency for CB6 glass at different temperatures.

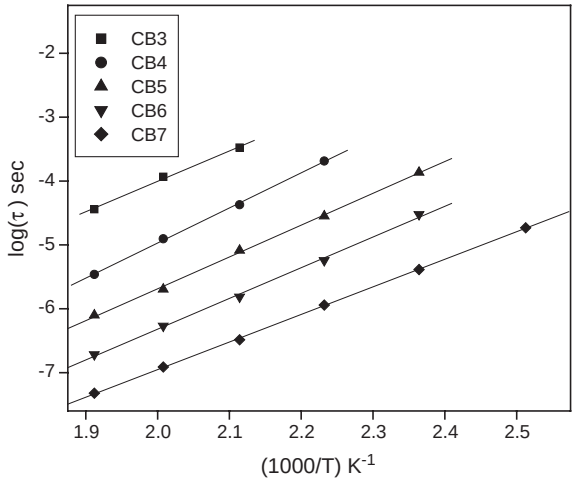

Fig. 7. Typical plot of $\log(\tau)$ versus $1000/T$ for CB glass series.

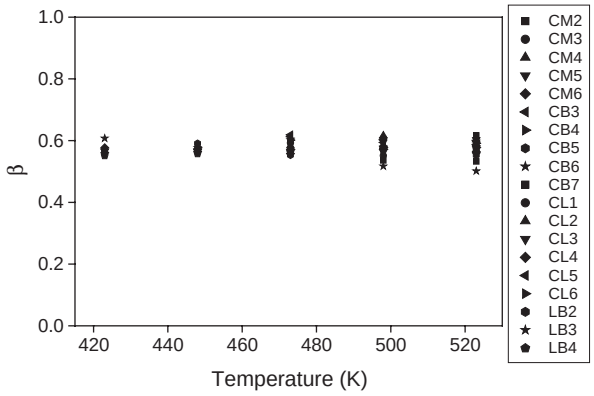

Fig. 8. Variation of β as a function of temperature for LB, CL, CM and CB series.

electrode polarization [25]. The real (M') and imaginary (M'') parts of dielectric moduli as a function of temperature and frequency for CB6 glass is shown in Fig. 6a and b. The behaviour of dielectric constant and dielectric modulus are qualitatively similar for all the glasses examined. It is evident from Fig. 6b that M'' values exhibit characteristically asymmetric peaks. The asymmetric M'' peak originates from the nature of relaxation behaviour. The center of the relaxation peak is characterized by f_o. It can also be seen from Fig. 6b that the M'' is found to be constant (M''_{max}) and the peaks systematically shift towards higher frequencies with increase of temperature. M'' peaks are reasonably well fitted using Kohlrausch–Williams–Watts (KWW) or stretched exponential function [26–28] for relaxation;

$$\phi = \phi_0 \exp\left[-\left(\frac{t}{\tau}\right)^{\beta}\right] \tag{10}$$

where τ is the characteristic relaxation time and β is the stretched exponent and its value lies between 0 and 1. The relaxation time τ_p was calculated using the relaxation

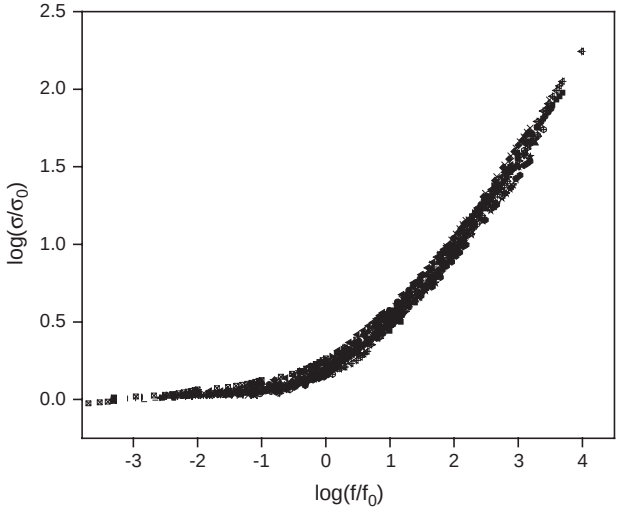

Fig. 9. Typical plots of $\log(\sigma/\sigma_o)$ versus $\log(f/f_o)$ for CL glass series between 423 K to 523 K.

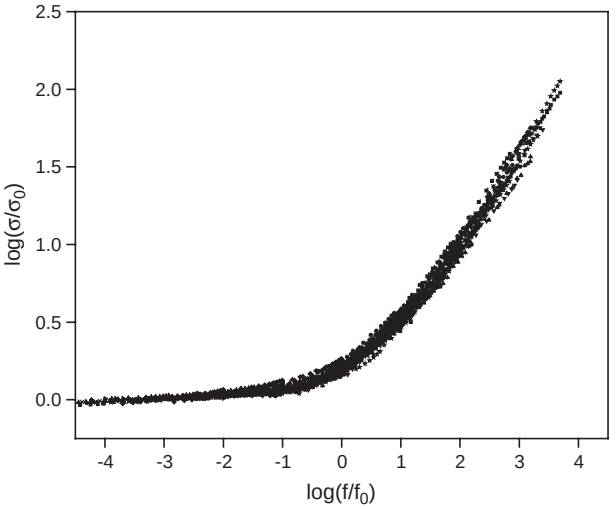

Fig. 10. Typical plot of $\log(f/f_o)$ versus $\log(\sigma/\sigma_o)$ for all the glass samples at different temperatures.

frequency (ω_p); $\tau_p = 1/\omega_p$. The relaxation time also systematically shifts to higher values with increase of temperature. The variation of $\log(\tau_p)$ versus $(1000/T)$ of LB, CL, CM and CB glass follow Arrhenius behaviour. A typical plot for CB glass series is shown in Fig. 7.

The characteristic relaxation time, τ_p is given by the relation,

$$\tau_p = \tau_0 \exp\left[\frac{E_{ac}}{kT}\right] \tag{11}$$

The values of ac activation energies, E_{ac} are given in Table 1 and it is observed that both E_{ac} and E_{dc} are almost same. This could be an indication of the fact that the ionic motion responsible for relaxation, diffusion independent and for diffusive motion are the same.

Full width at half maximum (FWHM) values of M'' peaks are inversely correlated to the values of β. Using

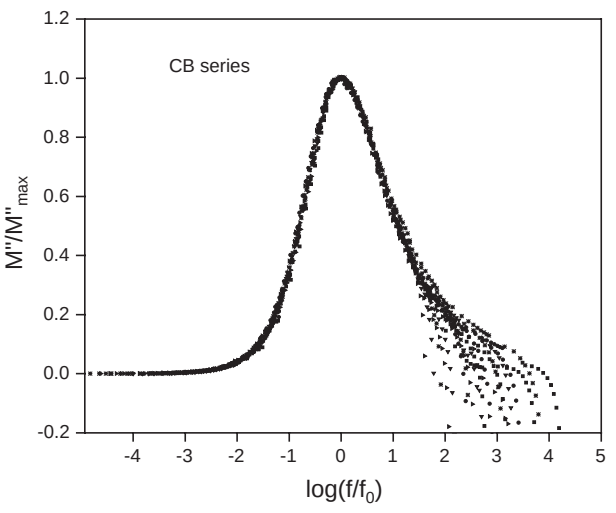

Fig. 11. Normalized plots of dielectric modulus against normalized frequency for CB glass series.

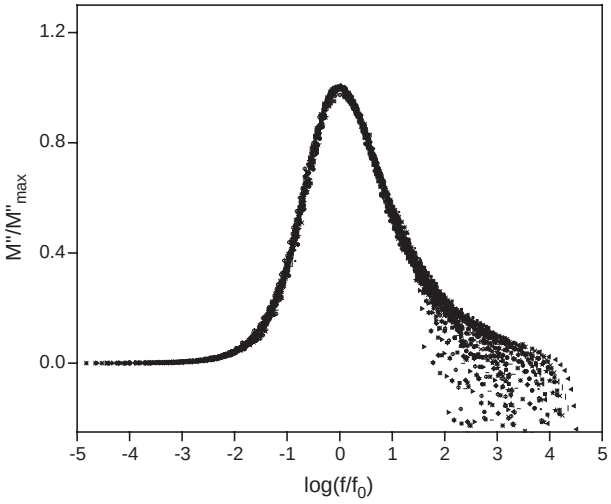

Fig. 12. Normalized plots of dielectric modulus against normalized frequency for all glass samples at different temperatures.

plots of β versus FWHM [25,29], β values have been evaluated for all the glasses at various temperatures and are plotted in Fig. 8 as a function of temperature. The β values investigated for all the glasses are found to be constant and lie in the narrow range of 0.5–0.6 and are essentially temperature insensitive. In the present glasses the relatively greater dependence of s and weak dependence of β on temperature is suggestive that β and s are not related in any simple complementary such as $\beta+s=1$ [20].

8. Normalized plots of conductivity and dielectric modulus

To examine the fact that the mechanism of ion transport in these glasses remains unaffected by composition and temperature, normalized plots of conductivity and imaginary part of dielectric modulus have been studied using the reduced (master) plots. The typical reduced plots of conductivity ($\log(\sigma/\sigma_o)$) versus frequency ($\log(f/f_o)$) for CL glass series are shown in Fig. 9. Similarly the log (σ/σ_o) versus $\log(f/f_o)$ plots for all the glass series and at different temperatures are plotted on a single graph. The data is found to be scaled very well and are shown in Fig. 10.

The reduced imaginary part of dielectric modulus (M''/M''_{max}) has been plotted as a function of $\log(f/f_o)$ and is shown in Fig. 11 for CB glasses, where M''_{max} is the maximum value of M'' in M'' versus $\log(f)$ plots. The variation of M''/M''_{max} versus $\log(f/f_o)$ for all the glass series is shown in Fig. 12. It is seen from Fig. 12 that the dielectric relaxation data also collapses excellently (M''/M''_{max} versus $\log(f/f_o)$) for the given range of temperatures. This suggests that the dynamical processes are temperature independent and the good time–temperature superposition shows that conduction mechanism remains unchanged and it is also indicative of a common ion transport mechanism, which operates in the entire range of composition and temperatures studied.

9. Conclusions

The conductivity studies of $Li_2O–MnO_2–B_2O_3$ glass system have been carried out over the wide range of frequency and temperature. The conductivity in this glass system is seen to be dominated by lithium ions and it is found to increase with increase of modifier concentration. AC conductivity data has been fitted to a single power law equation. The power law exponent s is found to decrease with increase of temperature and exhibit lower values in highly modified glasses. The stretched exponent factor β is found to be almost constant and it is independent of temperature. Scaling analysis of conductivity and dielectric modulus show excellent time–temperature superposition indicating common ion transport mechanism.

Acknowledgements

The authors are grateful to Professor K.J. Rao for encouragement and many discussions. One of the authors (R.V.A) acknowledges the UGC, Government of India for financial support to carry out this work.

References

[1] L.D. Pye, V.D. Frechette, N.J. Kreidl, Borate Glasses: Structure, Properties and Applications, Plenum Press, New York, 1978.
[2] H. Rawson, Inorganic Glass Forming Systems, Academic Press, London, 1967.
[3] J. Krogh-Moe, Phys. Chem. Glasses 3 (1962) 101.
[4] Su Fang, Solid State Ionics 7 (1982) 37.
[5] L. Chen, L. Wang, G. Che, G. Wang, Z. Li, Solid State Ionics 14 (1984) 149.
[6] D.L. Sidebottom, B. Roling, K. Funke, Phys. Rev., B 63 (2000) 24301.
[7] D.L. Sidebottom, P.F. Green, R.K. Brow, Phys. Rev., B 56 (1997) 170.
[8] K.J. Rao, Structural Chemistry of Glasses, Elsevier, 2002.
[9] A.H. Verhoef, H.W. den Hartog, Solid State Ionics 68 (1994) 305.
[10] S.I. Smedley, C.A. Angell, Mater. Res. Bull. 15 (1980) 421.
[11] H.L. Tuller, D.P. Button, D.R. Uhlmann, J. Non-Cryst. Solids 40 (1980) 93.
[12] D.E. Day, J. Non-Cryst. Solids 21 (1976) 343.
[13] S. Muthupari, S. Lakshmi Raghavan, K.J. Rao, J. Phys. Chem. 100 (1996) 4243.
[14] D.P. Almond, A.R. West, R.J. Grant, Solid State Commun. 44 (1982) 1277.
[15] D.P. Almond, G.K. Duncan, A.R. West, Solid State Ionics 8 (1983) 159.
[16] D.P. Almond, C.C. Hunter, A.R. West, J. Mater. Sci. 19 (1984) 3236.
[17] A.K. Jonscher, Nature 267 (1977) 673.
[18] K. Otto, Phys. Chem. Glasses 7 (1) (1966) 29.
[19] K.L. Ngai, J.N. Mundy, H. Jain, O. Kanert, G. Balzer-Jollenbeck, Phys. Rev., B 39 (1989) 6169.
[20] H.K. Patel, S.W. Martin, Phys. Rev., B 45 (1992) 10292.

[21] D.L. Sidebottom, J. Non-Cryst. Solids 244 (1999) 223.
[22] H. Jain, C.H. Hsieh, J. Non-Cryst. Solids 172 (1994) 1408.
[23] D.L. Sidebottom, J. Phys., Condens. Matter 15 (2003) S1585.
[24] O.L. Anderson, D.A. Stuart, J. Am. Ceram. Soc. 37 (1954) 573.
[25] C.T. Moynihan, L.P. Boesch, N.L. Laberge, Phys. Chem. Glasses 14 (1973) 122.
[26] R. Kohlrausch, Progg. Ann. Phys. 12 (1847) 393.
[27] G. Williams, D.C. Watts, Trans. Faraday Soc. 66 (1970) 80.
[28] G. Williams, D.C. Watts, S.B. Dev, A.M. North, Trans. Faraday Soc. 67 (1971) 1323.
[29] P.B. Macedo, C.T. Moynihan, R. Bose, Phys. Chem. Glasses 13 (1972) 171.